



**New insights into developing antibiofouling surfaces for industrial photobioreactors**

Journal:	<i>Biotechnology and Bioengineering</i>
Manuscript ID	19-189.R1
Wiley - Manuscript type:	Article
Date Submitted by the Author:	n/a
Complete List of Authors:	Zeriouh, O.; Universidad de Almeria, Chemical Engineering Rocamora-Marco, Arturo; Universidad de Almeria, Chemical Engineering Reinoso-Moreno, José Vicente; Universidad de Almeria, Chemical Engineering López-Rosales, Lorenzo; Universidad de Almeria, Chemical Engineering García, Francisco; University of Almeria, Chemical Engineering Grima, Emilio; University of Almeria, Chemical Engineering
Key Words:	Microalga, Photobioreactor, Anti-biofouling, Fouling Release Coatings, Biocompatibility theory

SCHOLARONE™  
Manuscripts

This is the peer reviewed version of the following article: [*Zeriouh, O., Marco-Rocamora, A., Reinoso-Moreno, J. V., López-Rosales, L., García-Camacho, F., and Molina-Grima, E. (2019). New insights into developing antibiofouling surfaces for industrial photobioreactors. Biotechnology and Bioengineering, 116(9), 2212-2222.*], which has been published in final form at <https://doi.org/10.1002/bit.27013>. This article may be used for non-commercial purposes in accordance with Wiley Terms and Conditions for Use of Self-Archived Versions. This article may not be enhanced, enriched or otherwise transformed into a derivative work, without express permission from Wiley or by statutory rights under applicable legislation. Copyright notices must not be removed, obscured or modified. The article must be linked to Wiley's version of record on Wiley Online Library and any embedding, framing or otherwise making available the article or pages thereof by third parties from platforms, services and websites other than Wiley Online Library must be prohibited."

1  
2  
3 **1 New insights into developing antibiofouling surfaces for industrial**  
4  
5 **2 photobioreactors**  
6  
7  
8  
9

10 4 O. Zeriouh<sup>1</sup>, A. Rocamora Marco<sup>1</sup>, J.V. Reinoso-Moreno<sup>1</sup>, L. López-Rosales<sup>1,2</sup>,  
11  
12 5 F. García-Camacho<sup>1,2</sup> and E. Molina-Grima<sup>1,2\*</sup>  
13

14 6 <sup>1</sup>Chemical Engineering Department, University of Almería, 04120 Almería, Spain  
15

16 7 <sup>2</sup>Research Center in Agrifood Biotechnology, University of Almería, 04120 Almería,  
17  
18 8 Spain  
19  
20

21 9  
22  
23  
24 10  
25  
26 11 \*Address correspondence to:  
27

28 12 E. Molina Grima, Chemical Engineering Department, University of Almería, 04120  
29  
30 13 Almería, Spain  
31

32 14 E-mail: emolina@ual.es  
33

34 15 Phone: 34-950015032  
35

36 16 Fax: 34-950015491  
37  
38  
39  
40 17

41  
42 18 Short running title: **Antibiofouling surfaces for photobioreactors**  
43  
44  
45 19

46  
47 20 Grant numbers: CTQ2013-46552-R; **CTQ2014-55888-C3-2-R**  
48

49 21 This is the [peer reviewed version](#) of the following article: [Zeriouh, O., Marco-Rocamora, A., Reinoso-Moreno,  
50 J. V., López-Rosales, L., García-Camacho, F., and Molina-Grima, E. (2019). *New insights into developing*  
51 22 *antibiofouling surfaces for industrial photobioreactors*. *Biotechnology and Bioengineering*, 116(9), 2212-2222.],  
52 which has been published in [final form at https://doi.org/10.1002/bit.27013](#). This article may be used for  
53 23 non-commercial purposes in accordance with Wiley Terms and Conditions for Use of Self-Archived  
54 Versions. This article may not be enhanced, enriched or otherwise transformed into a derivative work,  
55 24 without express permission from Wiley or by statutory rights under applicable legislation. Copyright notices  
56 must not be removed, obscured or modified. The article must be linked to Wiley's version of record on Wiley  
57 Online Library and any embedding, framing or otherwise making available the article or pages thereof by  
58 25 third parties from platforms, services and websites other than Wiley Online Library must be prohibited."  
59  
60

1  
2  
3 **26 Abstract**  
4

5 27 The biofouling formation of the marine microalga *N. gaditana* on non-toxic surfaces  
6  
7 28 was quantified on rigid materials, both coated (with Fouling Release Coatings and  
8  
9 29 nanoparticle coatings) and non-coated, to cover a wide range of surface properties from  
10  
11 30 strongly hydrophobic to markedly hydrophilic under conditions similar to those  
12  
13 31 prevailing in outdoor massive cultures of marine microalgae. The effect of seawater on  
14  
15 32 surfaces that presented the best antibiofouling properties was also evaluated. The  
16  
17 33 adhesion intensity on the different surfaces was compared with the predictions of the  
18  
19 34 biocompatibility theories developed by Baier and Vogler using water adhesion tension  
20  
21 35 ( $\tau^o$ ) as the quantitative parameter of surface wettability. For the most hydrophobic  
22  
23 36 surfaces,  $\tau^o \leq 0$ , the microalgae adhesion density increased linearly with  $\tau^o$ , following the  
24  
25 37 Baier's theory trend. However, for the rest of the surfaces,  $\tau^o \geq 0$ , a tendency towards  
26  
27 38 minimum adhesion was observed for amphiphilic surfaces with a  $\tau^o = 36 \text{ mJm}^{-2}$ , a value  
28  
29 39 close to that which minimizes cell adhesion according to Vogler's theory. The  
30  
31 40 understanding and combination of the two biocompatibility theories could help to  
32  
33 41 design universal antibiofouling surfaces that minimize the van der Waals forces and  
34  
35 42 prevent foulant adsorption by using a thin layer of hydration.  
36  
37  
38  
39  
40  
41  
42  
43  
44  
45  
46  
47  
48  
49  
50

51 47 Key words: Microalga; Photobioreactor; Anti-biofouling; Fouling Release Coatings;  
52  
53 48 Biocompatibility theory  
54  
55  
56  
57  
58  
59  
60

## 1. Introduction

Avoiding or delaying the appearance of biofouling in photobioreactors (PBRs) significantly lowers the costs of microalgal biomass production (Zerriouh et al., 2017a). Understanding the underlying phenomenology and fundamentals is essential for proposing solutions. Methodologies for determining the physicochemical properties of both the microalgae surface and the rigid materials that are potentially useful for fabricating PBRs used in the cultivation of planktonic marine microalgae have previously been developed (Zerriouh et al., 2017a; Zerriouh et al., 2017b; Zerriouh et al., 2019). In this context, the biocompatibility theories developed by Baier and Vogler (Vogler, 1998, 1999, 2001; Baier, 2006; Baier, 2014) may also help to design a universal antibiofouling surface for PBRs. Non-toxic hydrophobic Fouling Release Coatings (FRCs) exhibiting a critical surface tension ( $\gamma_c$ ) value near that which minimizes cell adhesion, ca. 22-24 mJm<sup>-2</sup> (hereinafter termed Baier's minimum), are currently considered to be the most promising environmentally friendly antifouling technology in the naval industry due to surface smoothness, low surface energy and a low modulus of elasticity that prompts adhered organisms to be released (Baier, 2006; Lejars et al., 2012). However, hydrophobic surfaces are also prone to protein adsorption and adhesion of certain microorganisms (mainly diatoms and bacteria) due to *hydrophobic attractions* (Yoon et al., 1997; Vogler, 2001). This has recently promoted research aimed at improving the anti-adhesion properties of Silicone-FRC coatings by increasing surface wettability using hydrophilic groups in the silicone matrix (Silicone-Amphiphilic coatings) (Galli & Martinelli, 2017; Wang & He, 2019). The amphiphilic surfaces with water adhesion tension ( $\tau^0$ ) values close to those that minimize cell adhesion, ca. 36 mJm<sup>-2</sup> (hereinafter named Vogler's minimum) present excellent antibiofouling properties compared to the low energy surfaces (LES) located at Baier's

1  
2  
3 76 minimum (Seetho et al., 2015). Currently, the Silicone-FRC coatings, which incorporate  
4  
5 77 amphiphilic block copolymers (mainly PEG-PDMS), are a good commercial non-toxic  
6  
7 78 alternative to prevent biofouling in marine environments, especially under **dynamic**  
8  
9 79 **conditions** (Camós-Noguer et al., 2017). These materials, both transparent and opaque,  
10  
11 80 could be respectively a promising alternative for fabricating closed and open PBRs,  
12  
13 81 where biofouling formation has not yet been well studied. In this work, the biofouling  
14  
15 82 of the microalga *N. gaditana* was quantified on non-toxic rigid material surfaces, both  
16  
17 83 coated (with FRCs and nanoparticle coatings) and non-coated, to cover a wide range of  
18  
19 84 surface properties from strongly hydrophobic to markedly hydrophilic surfaces under  
20  
21 85 conditions similar to those prevailing in outdoor massive microalgae cultures. The  
22  
23 86 effect of natural seawater on the  $\tau^o$  of surfaces that presented better antibiofouling  
24  
25 87 properties was also evaluated. The adhesion intensity of the *N. gaditana* microalgae on  
26  
27 88 the different surfaces was compared with the biocompatibility theory predictions  
28  
29 89 developed both by Baier and by Vogler using  $\tau^o$  as the quantitative parameter of surface  
30  
31 90 wettability.  
32  
33  
34  
35  
36  
37  
38  
39

## 40 92 **2. Materials and Methods**

### 41 93 *2.1 Photobioreactors and methods used to monitor the culture parameters*

42 94 The microalga used was *N. gaditana* B-3. The strain was provided by the Marine  
43 95 Culture Collection at the Andalusian Institute of Marine Sciences (CSIC, Cádiz, Spain).  
44 96 The culture medium consisted of natural seawater supplemented with macro and  
45 97 micronutrients. The exact composition of the culture medium is described elsewhere  
46 98 (Zeriouh et al., 2017b). A glass bench-scale flat-panel photobioreactor (FP-PBR) was  
47 99 used for the indoor experiments. The operational details and the dimensions of the FP-  
48 100 PBR have been described elsewhere (Zeriouh et al., 2019). The FP-PBR has a 13 L  
49  
50  
51  
52  
53  
54  
55  
56  
57  
58  
59  
60

1  
2  
3 101 volume; it is illuminated with artificial light 12h/24h and operated in continuous mode  
4  
5 102 at a dilution rate of 0.3 day<sup>-1</sup>.  
6

7  
8 103 In contrast, the outdoor experiments were carried out in a 7.2 m<sup>2</sup>, 900 L, pilot-scale  
9  
10 104 open raceway pond (RW). The operational details and the dimensions of this RW have  
11  
12 105 been previously reported (San Pedro et al., 2015). The culture circulated continuously  
13  
14 106 along the photobioreactor channels at an average velocity of 35 cms<sup>-1</sup>, driven by a  
15  
16 107 stainless-steel paddlewheel (0.60 m in diameter). The RW was inoculated with  
17  
18 108 exponential-phase inoculum grown and operated in semicontinuous mode. Filtered fresh  
19  
20 109 water was added to the RW to replace the amount of evaporated water. Each week, 750  
21  
22 110 L of fresh culture medium was supplied to the RW and the same volume of culture was  
23  
24 111 harvested. The experimental plan was carried out over July and August 2017. The  
25  
26 112 average temperature of the culture was approximately 29.0 °C and the mean irradiance  
27  
28 113 value was 2100 μE m<sup>-2</sup>·s<sup>-1</sup> (San Pedro et al., 2015).  
29  
30  
31  
32

33 114 The cell status of the cultures was checked daily by measuring the maximum  
34  
35 115 photochemical yield of the photosystem II (PSII), Fv/Fm, ratio with a fluorometer  
36  
37 116 (Mini-PAM-2500). The nitrate and phosphate concentrations dissolved in the  
38  
39 117 supernatant and the biomass concentration in the cultures were determined  
40  
41 118 spectrophotometrically as described earlier (Zeriouh et al., 2017b; Zeriouh et al., 2019).  
42  
43 119 Additionally, flow cytometry was used to quantify the cultures' cell density (cells mL<sup>-1</sup>).  
44  
45 120 The measurements were made using a Cell Lab Quanta SC flow cytometer (Beckman  
46  
47 121 Coulter Inc., Brea, CA, USA) equipped with an argon-ion excitation laser (blue light,  
48  
49 122 488 nm). At least 60,000 cells were analysed per sample. The flow rate was kept at a  
50  
51 123 moderate setting (data rate = 600 events s<sup>-1</sup>) to prevent interference between cells.  
52  
53  
54  
55

56 124

57  
58 125 *2.2 Preparation of both solid substrata and coatings for the adhesion test*  
59  
60

1  
2  
3 126 The average surface roughness ( $R_a$ ) (or arithmetic average deviation from the mean  
4  
5 127 line within the assessment length) was determined using a surface profiler (Dektak 150,  
6  
7  
8 128 Veeco Instruments Inc., USA) with 1 mm scan length and a 0.111  $\mu\text{m}/\text{sample}$   
9  
10 129 resolution. The  $R_a$  values for each surface are the average of several measurements (five  
11  
12 130 and eight for indoor and outdoor sample surfaces, respectively) from different sites on  
13  
14 131 each surface. Table 1 displays the  $R_a$  values of all the surfaces tested. A surface is  
15  
16  
17 132 considered smooth for  $R_a$  values below 0.6  $\mu\text{m}$ .

18  
19 133 In the case of the **outdoor pilot-plant experiments**, a rigid commercial  
20  
21 134 polycarbonate sheet ( $R_a=0.014\pm 0.004 \mu\text{m}$ ) was used as the solid support for the  
22  
23 135 application of the coatings. Thus, five square pieces (13cm x 13cm x 0.5cm) were  
24  
25 136 washed with Alconox detergent (1%) in ultrasound for 15 min, then rinsed with  
26  
27 137 abundant deionized water. The five clean square pieces were then dried at room  
28  
29 138 temperature for one day. One of the square pieces served as the control (a smooth  
30  
31 139 surface). Another piece was scratched with a wire brush (a Sealey WB05Y Stainless  
32  
33 140 Steel Wire Brush with a Plastic Handle) to create a rough surface ( $R_a=1.7 \mu\text{m}$ ). The  
34  
35 141 other three pieces were prepared using the following commercially available coatings:  
36  
37 142 (i) an antibiofouling FRC based on Silicone-Hydrogel technology (SilicOne®, Hempel,  
38  
39 143 Kongens Lyngby, Denmark) (C1); (ii) a superhydrophobic and oleophobic coating that  
40  
41 144 creates a surface chemistry and a texture thanks to the lotus effect caused by the  
42  
43 145 nanostructure of the product's particles (Ultra-Ever Dry®, UltraTech International, Inc.,  
44  
45 146 Florida, USA) (C2); and (iii) a hydrophobic coating with anti-adherent properties based  
46  
47 147 on nanoparticles (Plexiclean®, Nano-Care AG. Saarwellingen, Germany) (C3). The C1  
48  
49 148 coating was applied onto one of the square pieces of polycarbonate by means of bar-  
50  
51 149 coating surfaces to obtain a dry, homogeneous and smooth film with an approximate  
52  
53 150 thickness of 50  $\mu\text{m}$ . The two other coatings, C2 and C3, were applied onto the  
54  
55  
56  
57  
58  
59  
60

1  
2  
3 151 remaining two pieces of polycarbonate using an airbrush gun (Fengda® BD-180K, Art  
4  
5 152 & Hobby, s.c.o. Praga. The Czech Republic). **According to recommendations from**  
6  
7 153 **manufacturers**, during application, the air pressure was fixed at 4 bar and the coating  
8  
9 154 was dispersed through a 0.25mm-diameter nozzle. The pieces coated with C1, C2 and  
10  
11 155 C3 were dried at room temperature for 3 days and washed with abundant deionized  
12  
13 156 water. The  $R_a$  values measured for the three resulting surfaces PC-C1, PC-C2 and PC-  
14  
15 157 C3 **are shown in Table 1.**

16  
17  
18  
19 158 For the **indoor experiments**, six rigid materials with smooth surfaces were used  
20  
21 159 (Zeriouh et al., 2019): polyvinylchloride (PVC), polycarbonate (PC), polystyrene (PS),  
22  
23 160 borosilicate glass (GL), stainless steel (SS) and polyethylene (PE). These materials were  
24  
25 161 supplied in the form of 7.88mm-diameter disk coupons (Tyler Research Corp,  
26  
27 162 Edmonton, Canada) compatible with the Modified Robbins Device (MRD) flow  
28  
29 163 channel (LPMR-12PMMA, Tyler Research Corp, Edmonton, Canada). In addition,  
30  
31 164 eight PC disk coupons were coated with the coatings mentioned above (C1, C2 and C3)  
32  
33 165 and with Hempasil X3® (Hempel, Kongens Lyngby, Denmark) (C4). Hempasil X3® is  
34  
35 166 another non-toxic FRC that provides an invisible antibiofouling hydrogel microlayer.  
36  
37 167 Coatings C1 to C4 were dispersed on the coupons using the protocol described in the  
38  
39 168 second paragraph of this section.  
40  
41  
42  
43  
44  
45  
46

### 47 170 *2.3 Physicochemical properties of the materials and coatings used.*

48  
49 171 The sessile drop technique, applied with a goniometer (Drop Shape Analyzer  
50  
51 172 DSA25, KRÜSS GmbH, Germany), was used to measure the contact angles on the  
52  
53 173 different rigid materials and the coatings mentioned in Section 2.2. Two polar liquids  
54  
55 174 (water and formamide) and another apolar liquid (diiodomethane) were employed as  
56  
57 175 reference liquids. For each surface, two different samples were used. Before measuring  
58  
59  
60



176 the contact angles, the coatings and rigid materials used in outdoor pilot-plant  
 177 experiments were washed with Alconox detergent (1%), then rinsed with abundant  
 178 deionized water and allowed to dry at room temperature. Meanwhile, the surfaces  
 179 prepared for the indoor experiments were washed according to the protocol previously  
 180 described (Zerrouh et al., 2019). Briefly, the disc coupon materials mounted in the MRD  
 181 were rinsed out by closed-circuit recirculating in hot water (40 °C) containing 1%  
 182 Alconox® at a shear rate of 300 s<sup>-1</sup>. Subsequently, they were washed with deionized  
 183 and sterilized water under the same conditions at room temperature. Next, a sodium  
 184 hypochlorite (5%) solution was passed through at the same shear rate. Finally, the  
 185 coupons were washed with abundant deionized and sterilized water.

186 The contact angles measured and the equations used for the quantification of the  
 187 different surface energy components ( $\gamma_s^{LW}$ ,  $\gamma_s^+$ ,  $\gamma_s^-$ ,  $\gamma_s^{AB}$ ) for each surface, and the  
 188 change in the free energy of cohesion ( $\Delta G_{\text{coh}}$ ) are explicitly explained in the  
 189 Supplementary Material Section. The  $\tau^o$  value on each surface was calculated by  
 190 multiplying the water surface tension ( $\gamma_w = 72.8 \text{ mJm}^{-2}$ ) by the water's contact angle  
 191 cosine ( $\theta_w$ ) on this surface (Vogler, 1998); this being:

$$\tau^o = \gamma_w \cdot \cos \theta_w \quad [1]$$

192 The determination of  $\gamma_c$ , as defined by Zisman (1964), is valid for completely apolar  
 193 liquids (Van Oss, 1993). However, Van Oss (1993) reported that, for apolar surfaces,  $\gamma_c$   
 194 was equal to the apolar component of the surface free energy ( $\gamma_s^{LW}$ ) calculated using the  
 195 equation developed by Van Oss et al. (1988):

$$1 + \cos \theta = 2\sqrt{\gamma_s^{LW} / \gamma_L} \quad [2]$$

1  
2  
3 196 where  $\theta$  and  $\gamma_L$  are the contact angle and surface tension of the apolar liquid (i.e.,  
4  
5 197 diiodomethane), respectively. In our work, this approach has been adopted to determine  
6  
7  
8 198  $\gamma_c$  for all the different hydrophobic materials used.  
9

10 199

#### 12 200 *2.4 Toxicity assessment of the different coatings used*

14 201 Transparent 250 mL poly(propylene) cylindrical beakers, with a 70mm internal  
16 202 diameter, were used as culture vessels. The beakers were cleaned in an ultrasound bath  
18 203 for 15 minutes with detergent (Alconox, 1%), rinsed with abundant deionized water and  
20 204 dried at room temperature. Subsequently, the different coatings were applied to the  
22 205 interior of the clean beakers **by means of a paint brush**. Finally, the coated beakers were  
24 206 inoculated with a 100 mL culture volume of *N. gaditana* at a biomass concentration of  
26 207  $0.1 \text{ g L}^{-1}$  d.w. in exponential growth phase, using the same culture medium as described  
28 208 in Section 2.1. The beakers were then placed in an orbital shaker at 100 rpm. The  
30 209 cultures were grown under continuous illumination at  $25 \text{ }^\circ\text{C}$ , 12h/12h light-dark regime;  
32 210 this illumination being provided by 58W fluorescent lamps rendering an average  
34 211 irradiance on the culture vessel surface of  $135 \text{ } \mu\text{mol photons m}^{-2}\text{s}^{-1}$ . Clean beakers were  
36 212 used as the control (CT1) for the transparent coatings (C2 and C3). Meanwhile, the  
38 213 control beaker for the opaque coating (C1) was coated on the outside with an opaque  
40 214 **black** adhesive tape, **available commonly in stationery stores**, (CT2). In addition, a toxic  
42 215 matrix coating based on copper oxide (Hard racing TecCel®, Hempel) was used as the  
44 216 negative control. The tests were performed in duplicate. The monitoring of the biomass  
46 217 concentration ( $\text{gL}^{-1}$ ) and the Fv/Fm in each culture was carried out using the same  
48 218 methodology as described in Section 2.1. Cell viability was determined by a  
50 219 fluorescence staining assay in diacetate (FDA) (Xiao et al., 2011). Cells stained with  
52 220 FDA were detected in the FL1 channel of the flow cytometer. The optimal FDA  
54  
56  
58  
59  
60

1  
2  
3 221 concentration and exposure time for the culture samples in darkness was  $3 \times 10^{-3} \mu\text{g}$   
4  
5 222  $\text{mL}^{-1}$  and 15 min, respectively.  
6  
7  
8 223

9  
10 224 *2.5. Adhesion modules*  
11

12 225 The adhesion module for the **indoor** experiments comprised a modified Robbins  
13  
14 226 device (MRD) flow channel (LPMR-12PMMA, Tyler Research Corp, Edmonton,  
15  
16 227 Canada) with a 12.5mL volume and a peristaltic pump (Masterflex® L/STM Economy  
17  
18 228 drive) to allow culture broth from the PBR or seawater from a tank to be pumped into  
19  
20 229 the MRD. More details of the MRD can be found elsewhere (Zeriouh et al., 2019).  
21  
22 230 Briefly, the MRD contained 12 evenly-spaced ports which held sample holders with  
23  
24 231 recesses at the ends, into which the test disc coupons of the material or coating to be  
25  
26 232 studied were inserted. Before using the MRD, it was prepared as indicated earlier  
27  
28 233 (Zeriouh et al., 2019).  
29  
30  
31  
32

33 234 For the **outdoor** experiments, the adhesion assessment was performed on the five  
34  
35 235 polycarbonate sheets described in Section 2.2 (PC, rugged-PC, and PC coated with C1,  
36  
37 236 C2 and C3) attached to the bottom of a 900 L RW.  
38  
39  
40  
41

42 238 *2.6. Measurements of the physicochemical properties of the materials and coatings*  
43  
44 239 *exposed to natural seawater*  
45

46 240 The eight 7.88 mm-diameter polycarbonate disk coupons coated with the C1, C2,  
47  
48 241 C3 and C4 (see Section 2.2) coatings, together with two other uncoated PVC coupons,  
49  
50 242 were placed in the MRD holders. The adhesion module was connected to a storage tank  
51  
52 243 containing 1000 L of filtered seawater ( $0.45\mu\text{m}$ ) by means of silicone rubber tubes, and  
53  
54 244 the seawater was continuously pumped through the MRD at a flow rate of  $25 \text{ Lh}^{-1}$ . The  
55  
56 245 MRD output was directly connected to the drain. The drained volume (600 L) was  
57  
58  
59  
60

1  
2  
3 246 replaced daily. Both coated and uncoated coupons were continuously exposed to  
4  
5 247 seawater for six days. On the seventh day, the adhesion module was disconnected and  
6  
7 248 the coupons were disassembled from the MRD flow cell. They were then rinsed and  
8  
9  
10 249 dried at room temperature and the contact angles of the water on these surfaces were  
11  
12 250 measured according to the protocol described in Section 2.3.  
13  
14  
15 251

## 16 252 *2.7 Adhesion tests and biofouling quantification*

17  
18  
19 253 **Indoor experiments.** The six rigid and smooth materials (PVC, PC, PS, GL, SS  
20  
21 254 and PE) described in Section 2.2 were placed alternately in duplicate in the MRD flow  
22  
23 255 cell. After washing and sterilizing, the MRD was connected in a closed loop to the FP-  
24  
25 256 PBR, which was operated in continuous operational mode at a dilution rate of  $D=0.3$   
26  
27 257  $\text{day}^{-1}$ . This meant that the culture concentration that circulated through the MRD was  
28  
29 258 virtually the same during the entire experiment ( $2.5 \times 10^8 \text{ cell mL}^{-1}$ ). The culture flow  
30  
31 259 rate that circulated continuously through the MRD was  $25 \text{ Lh}^{-1}$ . In continuous culture  
32  
33 260 mode, the MRD was disconnected from the FP-PBR every two days, washed gently  
34  
35 261 with sterile seawater and then the density of the adhered cells per unit area ( $B$ ) on each  
36  
37 262 of the coupons ( $\text{cells cm}^{-2}$ ) was quantified, as previously described (Zerriouh et al.,  
38  
39 263 2017b; Zerriouh et al., 2019). These were then placed again in the MRD and reconnected  
40  
41 264 to the FP-PBR for the next measurements.  
42  
43  
44  
45

46  
47 265 **Outdoor pilot-plant experiments.** The five square pieces described above in  
48  
49 266 Section 2.2 were glued to the bottom of the open pond raceway photobioreactor (RW)  
50  
51 267 before being inoculated. After two months operating in semicontinuous mode, the  
52  
53 268 culture was removed from the RW. To eliminate the biological material deposited by  
54  
55 269 gravity on the pieces, the RW was immediately filled with filtered seawater, which was  
56  
57 270 circulated through the RW channels for 24 hours at the same flow rate as that used  
58  
59  
60

1  
2  
3 271 during the culture period ( $35 \text{ cm s}^{-1}$ ). Once the RW had been emptied, the square pieces  
4  
5 272 were photographed to compare the intensity of the biofouling formation on their  
6  
7 273 surfaces.  
8  
9

10 274

## 11 275 *2.8 Statistical analyses*

12  
13  
14 276 Statgraphics Centurion XVII (version 17.2.04) statistical software (2014, Statpoint  
15  
16  
17 277 Technologies, Inc. USA) was used for: (i) a significant difference analysis with a one-  
18  
19 278 way ANOVA test (ii) a significant difference analysis with a multi-way ANOVA test.  
20

21 279

## 22 280 **3. Results and discussion**

### 23 281 *3.1 Physicochemical characterization of the tested surfaces*

24  
25  
26 282 Table 1 shows the average surface roughness (Ra), the contact angles ( $\theta$ ), the total  
27  
28 283 free surface energy components ( $\gamma_s^{TOT}$ ), the free energy of cohesion ( $\Delta G_{coh}$ ) and the  
29  
30  
31 284 water adhesion tension ( $\tau^o$ ) of the different surfaces tested (see the calculation details in  
32  
33 285 the Supplementary Materials Section). The negative variation in the free energy of  
34  
35 286 cohesion ( $\Delta G_{coh} < 0$ ) of the different uncoated polymeric materials (PVC, PS, PE, PC),  
36  
37 287 the coated PC-C1, PC-C2 and PC-C3 and the stainless steel (SS) indicates that all these  
38  
39 288 surfaces are hydrophobic. It should be noted that two surfaces (PC-C2 and PC-C3) are  
40  
41 289 very low energy ( $2.4$  and  $11.9 \text{ mJm}^{-2}$ ) and have a very hydrophobic character compared  
42  
43 290 to the rest of the surfaces. This characteristic may be due to their special surface texture,  
44  
45 291 which is attributed to the nanoparticles. The glass (GL) surface is hydrophilic ( $\Delta G_{coh}$   
46  
47 292  $> 0$ ). The parameter  $\tau^o$ , an index of water reactivity with surfaces (Vogler, 1998), is  
48  
49 293 also included in Table 1. Surfaces with values of  $\tau^o \leq 0$  less than zero (i.e., PC- C1, PVC,  
50  
51 294 PS, and PE) can be considered **pure** hydrophobic surfaces (Vogler, 1998) (note that PC  
52  
53 295 is not purely hydrophobic – although  $\Delta G_{coh} < 0$ , according to Vogler (Vogler, 1998) its  
54  
55  
56  
57  
58  
59  
60

1  
2  
3 296  $\tau^o(=8.9 \text{ mJm}^{-2})>0$ ). For these surfaces: (i) the apolar component of the surface free  
4  
5 297 energy ( $\gamma_s^{LW}$ ) increases proportionally with  $\tau^o$  and, (ii) the polar component of the  
6  
7 298 surface free energy ( $\gamma_s^{AB}$ ) is also related to  $\tau^o$  although  $\gamma_s^{AB}$  is one order of magnitude  
9  
10 299 lower than that of  $\gamma_s^{LW}$  for hydrophobic surfaces. However, for values of  $\tau^o>0$ ,  $\gamma_s^{LW}$  is  
11  
12 300 relatively similar for all surfaces (Vogler, 1998); for example, even though the  
13  
14 301 difference of  $\tau^o$  between the PC and GL is  $52 \text{ mJm}^{-2}$ , the value of  $\gamma_s^{LW}$  only increases by  
15  
16 302  $1.1 \text{ mJm}^{-2}$  while for values of  $\tau^o$  greater than zero (i.e., hydrophilic (GL) and to a lesser  
17  
18 303 extent the slightly hydrophobic (PC) surfaces), the polar component increases  
19  
20 304 considerably. Even though they are different concepts,  $\gamma_c$  and  $\tau^o$  are linearly related in  
21  
22 305 the ( $-40 \text{ mJm}^{-2} \leq \tau^o \leq 25 \text{ mJm}^{-2}$ ) Vogler range (Vogler, 1998) (Fig. 1). In the same Fig. 1,  
23  
24 306 the values of  $\gamma_c$  versus  $\tau^o$  have been presented for all the surfaces used in this work. One  
25  
26 307 can observe that the values of  $\gamma_c$  and  $\tau^o$  for the polymeric surfaces including (PC-C1,  
27  
28 308 PVC, PS, PE and PC) exhibit a very good linear correlation ( $\gamma_c = 0.28 \cdot \tau^o + 27.85$ ;  
29  
30 309  $r^2=0.99$ ) (Fig. 1). The hypothetical  $\gamma_c$  value of GL calculated from this linearity is  $44.6$   
31  
32 310  $\text{mJm}^{-2}$ , a value similar to those reported in the bibliography (Baier, 1970; Dexter et al.,  
33  
34 311 1975; Dexter, 1979; Meyer et al., 1988). In the case of SS ( $\gamma_c=21.7 \text{ mJm}^{-2}$ ;  $\tau^o=-2.5 \text{ mJm}^{-2}$ ),  
35  
36 312 it does not conform to the linearity observed for hydrophobic polymeric substrates.  
37  
38 313 We do not have a full explanation for this but it could be due to the metallic nature of  
39  
40 314 the material, perhaps the presence of electron donating groups that interact with the  
41  
42 315 water's hydrogen bonds; this might slightly decrease the contact angle.  
43  
44  
45  
46  
47  
48  
49  
50  
51

316

### 317 3.2 Toxicity assessment of the coatings used

318 For ruling out the possible toxicity of the coatings employed on the *N. gaditana*  
319 cultures, *N. gaditana* was exposed to these coatings in cylindrical beakers. The results  
320 based on the mean values of maximum photochemical yield of PSII  $F_v/F_M$  ( $F_r$ ), cell

1  
2  
3 321 viability ( $V_r$ ) and biomass yield ( $Cf_r$ ), measured at the end of the batch cultures and  
4  
5 322 relative to corresponding values obtained from controls, are displayed in Fig. 2. The  
6  
7 323 coatings C2 and C3, based on nanoparticles, are transparent and the results were  
8  
9 324 compared with the control uncoated beaker (CT1 in Fig. 2). By contrast, the opaque  
10  
11 325 coating C1 was compared with the control beaker entirely covered with a darkened and  
12  
13 326 non-transparent adhesive (CT2 in Fig. 2). Other opaque coating used as negative  
14  
15 327 control, Hard racing TecCel® (HRT in Fig. 2), was demonstrated to be really toxic for  
16  
17 328 *N. gaditana* (i.e.  $F_r$ ,  $V_r$  and  $Cf_r$  equal to zero in Fig. 2). It can be appreciated from Fig. 2  
18  
19 329 that there were not statistically significant differences between the coatings C1, C2 and  
20  
21 330 C3 and the corresponding controls (i.e. values of  $F_r$ ,  $V_r$  and  $Cf_r$  near to 1) indicating that  
22  
23 331 these coatings are not toxic for the microalgae after a long-term exposure.  
24  
25  
26  
27  
28  
29  
30

### 333 *3.3 Exposure of both PC-coated materials and non-coated PVC to natural sea water.*

#### 334 *Impact on the water adhesion tension ( $\tau^o$ )*

335 The Baier curve establishes an empirical relationship between  $\gamma_c$  and the  
336 bioadhesion strength (Baier, 2006) (see later in Fig. 5). The relevance of this curve is  
337 the establishment of a minimum biological adhesion on surfaces whose initial  $\gamma_c$  ranges  
338 from 20 to 30 mJm<sup>-2</sup> (*theta* surfaces, or low-energy surfaces, LES). The antibiofouling  
339 efficiency of an LES increases when its modulus of elasticity decreases ( $E$ ) (Lejars et  
340 al., 2012). The best fouling release surfaces are those with the lowest value of ( $\sqrt{\gamma_c E}$ )  
341 (Lejars et al., 2012). Currently, poly(dimethyl) siloxane elastomers (PDMS) are the best  
342 alternative for fabricating FRCs under **dynamic conditions** (Lejars et al., 2012).  
343 However, the adsorption of proteins and other foulants to these surfaces (namely  
344 *hydrophobic attraction*) are unavoidable and finally leads to the formation of a  
345 ``conditioning film`` on the original surface (Meyer et al., 1988; Baier, 2014). The

1  
2  
3 346 peculiarity of **some** LES, when in contact with seawater, is that they preserve the  $\gamma_c$   
4  
5 347 value **close to the initial value** (22-24 mJm<sup>-2</sup>) despite the formation of the conditioning  
6  
7 348 film (Meyer et al., 1988) (Fig. 3A). In marine environments, the high ionic strength of  
8  
9  
10 349 seawater compresses the electrical double layer surrounding the particles (proteins,  
11  
12 350 colloids, cell debris and foulants, etc); consequently, the electrostatic interactions  
13  
14 351 between these particles and the submerged surfaces are negligible (Zerriouh et al.,  
15  
16 352 2017a). Although the “hydrophobic attractions” (i.e., acid-base, AB, interaction as  
17  
18 353 driving forces) are responsible for the formation of the “conditioning film” on the LES  
19  
20 354 (Yoon et al., 1997), the absence of acceptor and donor electron groups on these surfaces  
21  
22 355 (due to their hydrophobic nature) prevents the formation of covalent bonds between the  
23  
24 356 conditioning film and the surface. Apparently, the union between the conditioning film  
25  
26 357 and the LES is controlled by Van der Waals interactions. Regardless of the nature of the  
27  
28 358 conditioning film, ( $\gamma_c$ ) is equal to ( $\gamma_s^{LW}$ ); therefore, the apolar component of the free  
29  
30 359 energy of adhesion is practically zero (i.e.,  $\Delta G_{adh}^{LW} \approx 0$ ) (see the Supplementary Material  
31  
32 360 Section). Consequently, the conditioning film was not firmly attached to the surface  
33  
34 361 (and was easily detached), nor was it homogeneous; i.e., part of the original surface  
35  
36 362 remains uncovered, which allows it to **keep** its  $\gamma_c$  value **near the initial one** (Meyer et al.,  
37  
38 363 1988). Curiously, the LES used in this work (C1, C4 and PVC in Table 1), **with initial  $\gamma_c$**   
39  
40 364 **between 22 and 24, retained  $\gamma_c$  values within the 25-29 mJm<sup>-2</sup> range after 6 days natural**  
41  
42 365 **seawater exposure (calculations can be made from the  $\tau^o$  values, obtained after washing,**  
43  
44 366 **displayed in Fig. 3B using the equation from Fig. 1  $\gamma_c = 0.28\tau^o + 27.85$ ).** These results  
45  
46 367 are in line with those reported for a LES based on a coating of dimethyl-dichlorosilane  
47  
48 368 (Meyer et al., 1988) (see Fig. 3A). In addition, the three surfaces lost wettability and  
49  
50 369 showed amphiphilic properties since  $\tau^o$  on these surfaces increased considerably to  
51  
52 370 values of 35, 23 and 38 mJm<sup>-2</sup>, respectively, after natural seawater exposure (see Fig.  
53  
54  
55  
56  
57  
58  
59  
60



371 3B). This value of  $\tau^o$  corresponds to the minimum biological interaction predicted by  
372 Vogler (amphiphilic surfaces corresponding to  $\tau^o=30 \text{ mJm}^{-2}$  and  $\theta_w=65^\circ$ ) (Vogler,  
373 2001). The point is discussed in detail later in Section 3.5. The partial loss of  
374 hydrophobicity after washing with the LES coatings (see Fig. 3B) indicates that (i) the  
375 surfaces slightly and permanently lose hydrophobicity after exposure to natural  
376 seawater, especially C4 and C1, and (ii) for PVC, the conditioning film does not affect  
377  $\gamma_c$  although influences on the degree of hydration mean that the surfaces with the  
378 conditioning film acquire amphiphilic properties. For the coatings C1 and C4, as  
379 expected, the silicone-hydrogel technology induces these coatings to acquire an  
380 amphiphilic character after exposure to natural sea water. This response is probably due  
381 to their surface reorganization rather than the conditioning film (an important question  
382 for future studies). On the other hand, after exposure to natural seawater, the very low  
383 hydrophobic surface (PC-C2) conserves its wettability, while PC-C3, also a very  
384 hydrophobic surface, does not conserve it (see Fig. 3B). Both coatings (C2 and C3), due  
385 to the special texture of the resulting surfaces, are very low energy surfaces (2.5 and  
386  $11.9 \text{ mJm}^{-2}$ , respectively) and are located on the left side (super hydrophobic surfaces)  
387 of the Baier curve and the left line in Vogler's theory (Type I biological response)  
388 (Vogler, 2001; Baier, 2014). It is therefore predictable that biofouling on these coatings  
389 would be greater than in LES, as can be observed in Fig. 4B.

390

### 391 3.4 Development of biofouling on different materials and coatings

392 **Indoor experiments.** The average adhesion density ( $B$ ) of *N.gaditana* on the  
393 different materials, when the photobioreactor was operated in continuous mode (i.e., at  
394  $D=0.3\text{day}^{-1}$  and at a steady-state biomass concentration of  $2.5 \times 10^{-8} \text{ cel mL}^{-1}$ ), is shown  
395 in Fig. 4A. The relationship between  $B$  and  $\gamma_c$  or  $\tau^o$  of the tested materials is not

1  
2  
3 396 proportional. One can observe that: (i) the adhesion density is minimal on the LES (i.e.:  
4  
5 397 PVC:  $\gamma_c=23.41 \text{ mJm}^{-2}$  and SS:  $\gamma_c=21.74 \text{ mJm}^{-2}$ ) and, (ii) it seems that there could be  
6  
7 398 minimum adhesion for materials with  $\gamma_c$  amongst those corresponding to the PC and the  
8  
9 399 GL (i.e., another minimum of adhesion on the zone of amphiphilic surfaces;  $\tau^o=35 \text{ mJm}^{-2}$ ).  
10  
11 400 In decreasing order, the maximum value of  $B$  was observed on the PE ( $B_{\max} =$   
12  
13 401  $1.17 \times 10^5 \text{ cells cm}^{-2}$ ) followed by the rest of the materials: PS (41% less), GL (64%  
14  
15 402 less), PC (68% less), SS (86% less) and PVC (92% less than PC).  
16  
17  
18

19 403 **Outdoor experiments.** During the two months that these experiments lasted, the  
20  
21 404 open raceway reactor was operated in semicontinuous mode (Fig. 4B). The culture  
22  
23 405 maintained a healthy photosynthetic state, the mean value of  $F_v/F_m$  for the experiments  
24  
25 406 was  $0.604 \pm 0.034$ . The biomass concentration before weekly harvesting varied from  
26  
27 407  $0.79\text{-}0.71 \text{ gL}^{-1}$ . The phosphates ( $\text{PO}_4^{3-}$ ) were totally consumed each week (i.e.,  $0.2 \text{ mM}$   
28  
29 408 at the start of the culture, or when adding fresh culture medium, and  $\sim 0 \text{ mM}$  just before  
30  
31 409 harvesting; i.e., after 7 days), while the consumption of nitrates was about 40% each  
32  
33 410 week. The nitrates concentration before weekly harvesting varied from  $10.4\text{-}11.8 \text{ mM}$   
34  
35 411 after an initial  $17.7 \text{ mM}$  at the start of the culture (or renewal). Following two months of  
36  
37 412 operation, the open reactor was emptied to evaluate the degree of biofouling on the  
38  
39 413 materials placed at the bottom of the RW. The coated PC-C1 showed a lower degree of  
40  
41 414 biofouling compared to the other materials and coatings (Fig. 4B). After washing, the  
42  
43 415 microalgal deposited on the PC-C1 surface was easily detached whereas the other  
44  
45 416 materials and coatings showed almost the same degree of biofouling as that observed  
46  
47 417 before these coupons were washed (Fig. 4B). The biological material deposited on PC-  
48  
49 418 C1 was clearly due to the culture sedimentation after emptying the RW while the  
50  
51 419 adhesion on the rest of the materials and coatings was irreversible. The photographs  
52  
53 420 (Fig. 4B) also demonstrate that the material's roughness plays an important role in  
54  
55  
56  
57  
58  
59  
60

1  
2  
3 421 biofilm development on the materials - the rugged polycarbonate (PC-rugged,  
4  
5 422  $R_a=1.69\pm0.41 \mu\text{m}$ ) showed more biofouling than the smooth polycarbonate (PC-control,  
6  
7 423  $R_a=0.014\pm0.004 \mu\text{m}$ ). The coated PC-C2, which is also a rugged surface, and PC-C3 did  
8  
9 424 not demonstrate good antibiofouling properties. The biofilm developed on PC-C3 was  
10  
11 425 like that on the PC-control piece. On the other hand, the microalgal adhesion to PC-C2  
12  
13 426 was still greater and very similar to the results obtained for the roughed-PC (note that  
14  
15 427 both PC-C2 and PC-C3 are on the left side of both Baier's curve (Baier, 2014) and the  
16  
17 428 Type I biological response of Vogler's theory (Vogler, 2001)). We do not have a  
18  
19 429 coherent explanation regarding the biofouling observed with these two nanoparticle-  
20  
21 430 based coatings (C2 and C3) but while the rugged surface PC-C2 continued to maintain  
22  
23 431 its highly hydrophobic character throughout the experiment, PC-C3 acquired a  
24  
25 432 hydrophilic character during its exposure to the marine culture medium in which the  
26  
27 433 tests were carried out, yet reacquired its hydrophobic character straight after washing  
28  
29 434 this surface (Fig. 3B).  
30  
31  
32  
33  
34  
35  
36

37 436 *3.5 How the surface biocompatibility theories of Baier and Vogler may help to develop*  
38  
39 437 *antifouling surfaces for microalgae photobioreactors*

40  
41  
42 438 Fig. 5 shows the two biocompatibility theories developed by Baier and Vogler that  
43  
44 439 relate relative biological interaction with solid surfaces in a wide range of wettability  
45  
46 440 (Vogler, 2001). Baier's theory predicts minimum biological interaction on hydrophobic  
47  
48 441 surfaces of low wettability ( $\gamma_c=22-24 \text{ mJm}^{-2}$ ,  $\theta_w=100^\circ-110^\circ$ ,  $\tau^\circ=15-17 \text{ mJm}^{-2}$ ). The  
49  
50 442 interaction strength increases in both directions; that is to say, when the hydrophobicity  
51  
52 443 increases and also when it decreases. Vogler's theory predicts minimum adhesion on  
53  
54 444 amphiphilic surfaces ( $\tau^\circ=35 \text{ mJm}^{-2}$ ,  $\theta_w=65^\circ$ ) (Vogler, 2001); here, it is possible to  
55  
56 445 distinguish between two types of responses: (i) Type I, which corresponds to the  
57  
58  
59  
60

1  
2  
3 446 adsorption of proteins on hydrophobic surfaces ( $\tau^o < 35 \text{ mJm}^{-2}$ ), with adhesion intensity  
4  
5 447 increasing in line with surface hydrophobicity, and (ii) Type II, which corresponds to  
6  
7 448 interfacial phenomena related to the physicochemical properties of the hydration layer  
8  
9  
10 449 on hydrophilic surfaces ( $\tau^o > 35 \text{ mJm}^{-2}$ ) favouring the adsorption of polyvalent  
11  
12 450 electrolytes that subsequently interact with proteins and cells – with the biological  
13  
14 451 interaction density increasing in line with the surface hydrophilicity.

15  
16  
17 452 The adhesion density ( $B$ ) on the different materials tested according to  $\tau^o$  has also  
18  
19 453 been included in Fig. 5. For the most hydrophobic surfaces, except for SS (i.e., PVC, PS  
20  
21 454 and PE), the value of  $B$  increases linearly with  $\tau^o$  in accordance with Baier's theory ( $r^2 =$   
22  
23 455  $0.99$ ;  $p < 0.05$ ) up to  $\tau^o \leq 0$ ; the minimum adhesion density was observed on the PVC  
24  
25 456 surface located at Baier's minimum ( $\gamma_c = 23.4 \text{ mJm}^{-2}$  and  $\tau^o = -15.41 \text{ mJm}^{-2}$ ). For the  $\tau^o \geq 0$   
26  
27 457 surfaces (PC and GL), the adhesion tendency could be adjusted to Vogler's theory,  
28  
29 458 which predicts a minimum of adhesion on the amphiphilic surfaces ( $\tau^o = 35 \text{ mJm}^{-2}$ ). In  
30  
31 459 the same figure, we have inserted the surface coated with C1, based on FRCs-Hydrogel,  
32  
33 460 which showed extraordinary antibiofouling properties. This surface, although initially  
34  
35 461 having LES properties ( $\gamma_c = 22 \text{ mJm}^{-2}$  and  $\tau^o = -21.2 \text{ mJm}^{-2}$ ), after exposure to sea water  
36  
37 462 acquires amphiphilic properties, which are located just at the Vogler minimum ( $\tau^o = 35$   
38  
39 463  $\text{mJm}^{-2}$ ). The PVC (located at Baier's minimum) also acquires amphiphilic properties  
40  
41 464 with a  $\tau^o$  value similar to that of C1 after being in contact with sea water for 6 days (see  
42  
43 465 Fig. 3B); this is probably due to the adsorption of glycoproteins, polysaccharides and  
44  
45 466 other foulants present in the natural sea water (Baier, 2006), which end up forming a  
46  
47 467 conditioning film that partially covers the original surface, giving it amphiphilic  
48  
49 468 properties. The nature of the conditioning film is dynamic (Vogler, 1999); therefore, for  
50  
51 469 long exposure times, biofouling development on chemically-induced amphiphilic  
52  
53 470 surfaces should be more efficient and stable than on amphiphilic conditioning film.  
54  
55  
56  
57  
58  
59  
60

1  
2  
3 471 The effectiveness of LES ( $\gamma_c = \gamma_s^{LW} = 22-24 \text{ mJm}^{-2}$ ) is mainly due to the minimal Van  
4  
5 472 der Waals interactions ( $\gamma_s^{LW} \approx \gamma_W^{LW} = 21.8 \text{ mJm}^{-2}$ ); however, the adsorption of proteins  
6  
7 473 due to *hydrophobic attractions* favours the formation of a “conditioning film”. The  
8  
9 474 effectiveness of amphiphilic surfaces lies in their dual character (hydrophobic-  
10  
11 475 hydrophilic) - the hydrophobic part minimizes Van der Waals interactions while the  
12  
13 476 polar part induces the formation of a hydration layer that reverses *hydrophobic*  
14  
15 477 *attractions* to hydrophilic repulsion (i.e., hydration repulsion) (Van Oss, 1993). In  
16  
17 478 addition, the low modulus of elasticity improves the antifouling characteristics of these  
18  
19 479 surfaces. **Nonetheless, microbial foulants at small length scales (e.g. microalgae,**  
20  
21 480 **bacteria, algal spores and proteins) have such an extremely low modulus that they are**  
22  
23 481 **incapable of deforming any reasonably robust solid substrate and thus the antibiofouling**  
24  
25 482 **effects of chemistry-based surface design approaches dominate (Halvey et al., 2018).**  
26  
27 483 **Therefore, consistent with our study, lowering the surface free energy should be in**  
28  
29 484 **general sufficient to reduce biofouling at this scale. An exception is some diatom**  
30  
31 485 **species. They possess a high modulus shell that could reach hundreds of GPa, requiring**  
32  
33 486 **surfaces with low modulus and fine-tuned chemistry for antifouling properties (Halvey**  
34  
35 487 **et al., 2018).**

36  
37 488 Although it has been demonstrated in this work that Hempasil X3® and SilicOne®  
38  
39 489 are excellent candidates for coating raceway PBR walls, more research is needed to  
40  
41 490 develop similar coatings, in terms of their physicochemical properties, but making them  
42  
43 491 transparent so that they can be used in the manufacture of closed PBRs.  
44

#### 492 493 **4. Conclusions**

494 Rigid materials with a smooth texture, FRCs coatings based on hydrogel and  
495 coatings based on nanoparticles were used to evaluate their antibiofouling properties in  
60

1  
2  
3 496 marine microalgae photobioreactors. The physicochemical properties of the original  
4  
5 497 surfaces tested varied from very hydrophobic to hydrophilic. The coatings used did not  
6  
7  
8 498 alter the growth, the photosynthetic efficiency or the cell viability of the microalga *N.*  
9  
10 499 *gaditana* even after several days of exposure. The LES ( $\gamma_c=22-24$  mJm<sup>-2</sup>) located at the  
11  
12 500 Baier minimum, lost their wettability after exposure to natural sea water and acquired  
13  
14 501 amphiphilic properties; probably due to the formation of a conditioning film, in the case  
15  
16  
17 502 of PVC, and the chemical composition of the surface, in the case of the FRCs-hydrogel  
18  
19 503 (Hempasil X3® and SilicOne®) coatings. The roughness of a surface favours adhesion  
20  
21 504 and the development of biofouling. The experimental data were adjusted to the  
22  
23  
24 505 biocompatibility theories developed by Baier and Vogler, where the best results were  
25  
26 506 observed on LES and amphiphilic surfaces; although, after exposure to natural seawater,  
27  
28 507 all these surfaces acquired an amphiphilic character.

508

### 509 **Acknowledgements**

510 This research was funded by the Spanish Ministry of Economy and Competitiveness  
511 Projects CTQ2013-46552-R and CTQ2014-55888-C3-02-R, and the European Regional  
512 **Development Fund Program**. O. Zeriuoh wishes to thank the Ministry of Economy and  
513 Competitiveness for the grant awarded to carry out the doctoral thesis. Special thanks to  
514 Benjamin Sierra for the roughness measurements and their discussion, and the  
515 representative of Hempel in Andalusia (Spain) for donating three of the coatings used in  
516 this work (SilicOne®, Hempasil X3® and Hard Racing TecCel®).

517

### 518 **Conflicts of Interest Statement**

519 The authors report no conflicts of interest

520

521 **Nomenclature**

522

523 *Acronyms*

524 C1 based-SilicOne® coating

525 C2 based-Ultra-Ever Dry® coating

526 C3 based- Plexiclean® coating

527 C4 based-Hempasil X3® coating

528 FDA fluorescein diacetate

529 FP-PBR laboratory-scale flat-panel photobioreactor

530 FRC fouling release coating

531 GL borosilicate glass

532 LES low energy surfaces

533 MRD modified robbins device

534 PBR photobioreactor

535 PC polycarbonate

536 PDMS poly(dimethylsiloxane)

537 PE polyethylene

538 PEG polyethylene glycol

539 PS polystyrene

540 PVC polyvinylchloride

541 RW-PBR pilot-scale race-way photobioreactor

542 SHT silicone hydrogels technology

543 SS stainless steel

544

545 *Variables and parameters*

1			
2			
3	546	$B$	microalgae adhesion intensity (cells m <sup>-2</sup> )
4			
5	547	$F_V$	maximum variable fluorescence of chlorophyll (au)
6			
7	548	$F_M$	maximum fluorescence of chlorophyll (au)
8			
9			
10	549	$R_a$	average roughness (μm)
11			
12	550		
13			
14			
15	551	<i>Greek symbols</i>	
16			
17	552	$\gamma$	surface free energy (J m <sup>-2</sup> )
18			
19			
20	553	$\gamma_c$	critical surface tension (J m <sup>-2</sup> )
21			
22			
23	554	$\Delta G$	change in free energy (J m <sup>-2</sup> )
24			
25	555	$\theta$	contact angle, °
26			
27	556	$\tau^\circ$	water adhesion tension, J m <sup>-2</sup>
28			
29			
30	557		
31			
32	558	<i>Superscripts</i>	
33			
34	559	$AB$	refers to acid–base, i.e. polar component
35			
36	560	$EL$	refers to electrostatic component
37			
38			
39	561	$LW$	refers to Lifshitz–van der Waals, i.e. apolar or dispersive component
40			
41	562	$TOT$	refers to the total sum of the all components ( $AB$ , $EL$ , $LW$ )
42			
43	563	+	refers to electron acceptor parameter
44			
45	564	-	refers to electron donor parameter
46			
47			
48	565		
49			
50	566	<i>Subscripts</i>	
51			
52	567	$coh$	refers to cohesion
53			
54			
55	568	$D$	refers to the probe liquid diiodomethane
56			
57	569	$F$	refers to the probe liquid formamide
58			
59	570	$s$	refers to substrate
60			



1  
2  
3 571 *W* refers to the probe liquid water  
4  
5  
6 572  
7  
8  
9 573  
10

11 574 **References**

12  
13  
14 575 Baier, R. E. (1970). Surface properties influencing biological adhesion. In R. S. Manly  
15  
16 576 (Ed.), *Adhesion in biological systems* (pp. 15-48). New York: Academic Press.

17  
18 577 Baier, R. E. (2006). Surface behaviour of biomaterials: the theta surface for  
19  
20  
21 578 biocompatibility. *Journal of Materials Science: Materials in Medicine*, 17(11),  
22  
23 579 1057. doi:10.1007/s10856-006-0444-8

24  
25 580 Baier, R. E. (2014). Correlations of materials surface properties with biological  
26  
27  
28 581 responses. *Journal of Surface Engineered Materials and Advanced Technology*,  
29  
30 582 5(1), 42-51. doi:10.4236/jseamat.2015.51005

31  
32 583 Camós-Noguer, A., Olsen, S.M., Hvilsted, S., & Kiil, S. (2017). Diffusion of surface-  
33  
34 584 active amphiphiles in silicone-based fouling-release coatings. *Progress*  
35  
36 585 *in Organic Coatings*, 106, 77-86. doi:10.1016/j.porgcoat.2017.02.014

37  
38  
39 586 Dexter, S., Sullivan, J., Williams, J., & Watson, S. (1975). Influence of substrate  
40  
41 587 wettability on the attachment of marine bacteria to various surfaces. *Applied and*  
42  
43 588 *Environmental Microbiology*, 30(2), 298-308.

44  
45  
46 589 Dexter, S. C. (1979). Influence of substratum critical surface tension on bacterial  
47  
48 590 adhesion—in situ studies. *Journal of Colloid and Interface Science*, 70(2), 346-  
49  
50 591 354. doi:10.1016/0021-9797(79)90038-9

51  
52  
53 592 Galli, G., & Martinelli, E. (2017). Amphiphilic polymer platforms: Surface engineering  
54  
55 593 of films for marine antibiofouling. *Macromolecular Rapid Communications*,  
56  
57 594 38(8), 1600704. doi:10.1002/marc.201600704  
58  
59  
60

- 1  
2  
3 595 Halvey, A. K., Macdonald, B., Dhyani, A., & Tuteja, A. (2018). Design of surfaces for  
4  
5 596 controlling hard and soft fouling. *Philosophical Transactions of the Royal*  
6  
7 597 *Society A*, 377(2138), 20180266. doi:10.1098/rsta.2018.0266
- 8  
9  
10 598 Lejars, M. n., Margailan, A., & Bressy, C. (2012). Fouling release coatings: a nontoxic  
11  
12 599 alternative to biocidal antifouling coatings. *Chemical Reviews*, 112(8), 4347-  
13  
14 600 4390. doi:10.1021/cr200350v
- 15  
16  
17 601 Meyer, A., Baier, R., & King, R. (1988). Initial fouling of nontoxic coatings in fresh,  
18  
19 602 brackish, and sea water. *The canadian journal of chemical engineering*, 66(1),  
20  
21 603 55-62. doi:10.1002/cjce.5450660108
- 22  
23  
24 604 San Pedro, A., González-López, C., Acién, F., & Molina-Grima, E. (2015). Outdoor  
25  
26 605 pilot production of *Nannochloropsis gaditana*: influence of culture parameters  
27  
28 606 and lipid production rates in raceway ponds. *Algal Research*, 8, 205-213.  
29  
30 607 doi:10.1016/j.algal.2015.02.013
- 31  
32  
33 608 Seetho, K., Zhang, S., Pollack, K. A., Zou, J., Raymond, J. E., Martinez, E., & Wooley,  
34  
35 609 K. L. (2015). Facile synthesis of a phosphorylcholine-based zwitterionic  
36  
37 610 amphiphilic copolymer for anti-biofouling coatings. *ACS Macro Letters*, 4(5),  
38  
39 611 505-510. doi:10.1021/mz500818c
- 40  
41  
42 612 Van Oss, C. (1993). Acid—base interfacial interactions in aqueous media. *Colloids and*  
43  
44 613 *Surfaces A: Physicochemical and Engineering Aspects*, 78, 1-49.  
45  
46 614 doi:10.1016/0927-7757(93)80308-2
- 47  
48  
49 615 Van Oss, C. J., Chaudhury, M. K., & Good, R. J. (1988). Interfacial Lifshitz-van der  
50  
51 616 Waals and polar interactions in macroscopic systems. *Chemical Reviews*, 88(6),  
52  
53 617 927-941. doi:10.1021/cr00088a006
- 54  
55  
56  
57  
58  
59  
60

- 1  
2  
3 618 Vogler, E. A. (1998). Structure and reactivity of water at biomaterial surfaces. *Advances*  
4  
5 619 *in Colloid and Interface Science*, 74(1-3), 69-117. doi:10.1016/S0001-  
6  
7 620 8686(97)00040-7  
8  
9  
10 621 Vogler, E. A. (1999). Water and the acute biological response to surfaces. *Journal of*  
11  
12 622 *Biomaterials Science, Polymer Edition*, 10(10), 1015-1045.  
13  
14 623 doi:10.1163/156856299X00667  
15  
16  
17 624 Vogler, E. A. (2001). How water wets biomaterials surfaces. In M. Morra (Ed.), *Water*  
18  
19 625 *in biomaterials surface science* (pp. 269-290). Chichester: John Wiley & Sons  
20  
21 626 Ltd.  
22  
23  
24 627 Wang, J., & He, C. (2019). Photopolymerized biomimetic self-adhesive  
25  
26 628 Polydimethylsiloxane-based amphiphilic cross-linked coating for anti-  
27  
28 629 biofouling. *Applied Surface Science*, 463, 1097-1106.  
29  
30 630 doi:10.1016/j.apsusc.2018.08.214  
31  
32  
33 631 Xiao, X., Han, Z.-y., Chen, Y.-x., Liang, X.-q., Li, H., & Qian, Y.-c. (2011).  
34  
35 632 Optimization of FDA-PI method using flow cytometry to measure metabolic  
36  
37 633 activity of the cyanobacteria, *Microcystis aeruginosa*. *Physics and Chemistry of*  
38  
39 634 *the Earth, Parts A/B/C*, 36(9-11), 424-429. doi:10.1016/j.pce.2010.03.028  
40  
41  
42 635 Yoon, R.-H., Flinn, D. H., & Rabinovich, Y. I. (1997). Hydrophobic interactions  
43  
44 636 between dissimilar surfaces. *Journal of Colloid and Interface Science*, 185(2),  
45  
46 637 363-370. doi:10.1006/jcis.1996.4583  
47  
48  
49 638 Zeriouh, O., Reinoso-Moreno, J., López-Rosales, L., Cerón-García, M., Mirón, A. S.,  
50  
51 639 García-Camacho, F., & Molina-Grima, E. (2019). Assessment of a  
52  
53 640 photobioreactor-coupled modified Robbins device to compare the adhesion of  
54  
55 641 *Nannochloropsis gaditana* on different materials. *Algal Research*, 37, 277-287.  
56  
57 642 doi:10.1016/j.algal.2018.12.008  
58  
59  
60

- 1  
2  
3 643 Zeriouh, O., Reinoso-Moreno, J., López-Rosales, L., Cerón-García, M., Sánchez-Mirón,  
4  
5 644 A., García-Camacho, F., & Molina-Grima, E. (2017a). Biofouling in  
6  
7 645 photobioreactors for marine microalgae. *Critical Reviews in Biotechnology*,  
8  
9 646 37(8), 1006-1023. doi:10.1080/07388551.2017.1299681  
10  
11  
12 647 Zeriouh, O., Reinoso-Moreno, J., López-Rosales, L., Sierra-Martín, B., Cerón-García,  
13  
14 648 M., Sánchez-Mirón, A., Fernández-Barbero, A., García-Camacho, F., & Molina-  
15  
16 649 Grima, E. (2017b). A methodological study of adhesion dynamics in a batch  
17  
18 650 culture of the marine microalga *Nannochloropsis gaditana*. *Algal Research*, 23,  
19  
20 651 240-254. doi:10.1016/j.algal.2017.02.008  
21  
22  
23 652 Zisman, W. A. (1964). Relation of the equilibrium contact angle to liquid and solid  
24  
25 653 constitution. *Advan. Chem. Ser.*, 43, 1-51. doi:10.1021/ba-1964-0043.ch001  
26  
27  
28 654  
29  
30  
31  
32  
33  
34  
35  
36  
37  
38  
39  
40  
41  
42  
43  
44  
45  
46  
47  
48  
49  
50  
51  
52  
53  
54  
55  
56  
57  
58  
59  
60

1  
2  
3 **Legends**  
4

5 **Fig. 1.** Comparison of the predicted relationship (dashed line) between the critical  
6 surface tension ( $\gamma_c$ ) and water adhesion tension ( $\tau^o$ ) reported by Vogler (1998) and the  
7 relationship (dotted line) obtained from the experimental data in this study (open and  
8 filled circles). The solid line indicates the relationship between  $\gamma_c$  and  $\tau^o$  for only the five  
9 polymeric and hydrophobic surfaces: (SilicOne®, PVC, PC, PS and PE – filled circles).  
10  
11  
12  
13  
14  
15  
16  
17  
18

19 **Fig. 2.** Evaluation of the toxicity of the coatings used based on the values of maximum  
20 photochemical yield of PSII ( $F_v/F_m$ ), cell viability ( $V_r$ ) and biomass yield ( $C_f$ ) reached  
21 at the end of batch cultures, relative to corresponding values obtained from controls  
22 (CT1 and CT2). Data points are averages, and vertical bars are standard deviation (SD)  
23 for duplicate samples. Points without SD bars indicate that the SD was smaller than the  
24 symbol.  
25  
26  
27  
28  
29  
30  
31  
32  
33  
34

35 **Fig. 3.** Effect of seawater exposure on the water adhesion tension ( $\tau^o$ ) and water contact  
36 angle ( $\theta_w$ ) of coatings and materials used. **(A)** Temporal evolution of the critical surface  
37 tension ( $\gamma_c$ ) of the low energy surfaces used in this study (SilicOne®, Hemptasil X3®  
38 and PVC) under exposure to seawater. (empty circles and dashed line represent data  
39 reported elsewhere (Meyer et al., 1988)). **(B)** Measurements of  $\theta_w$  and  $\tau^o$  on PVC, PC-  
40 C2 (Ultra-Ever Dry®), PC-C3 (Plexiclean®), PC-C1 (SilicOne®) and PC-C4  
41 (Hemptasil X3®) before exposition, after 6 days of exposure to seawater and after  
42 washed with distilled water. The hatched band indicates the range of values associated  
43 with amphiphilic surfaces.  
44  
45  
46  
47  
48  
49  
50  
51  
52  
53  
54  
55  
56  
57  
58  
59  
60

1  
2  
3 **Figure 4. (A)** Indoor experiments. Variation in the number of adhered cells per cm<sup>2</sup> (*B*)  
4  
5  
6 as a function of the critical surface tension ( $\gamma_c$ ) and water adhesion tension ( $\tau^o$ ) for  
7  
8 different materials tested in the MRD in contact with the culture of *N. gaditana*. The  
9  
10 culture was boosted from the PBR module, operated in continuous operational mode, at  
11  
12 a flow rate of 25 L h<sup>-1</sup> providing fluid-dynamics conditions in the boundary layer of the  
13  
14 tested materials similar to those existing in the vicinity of the wall of a tubular PBR.  
15  
16 Lowercase letters indicate values that did not differ significantly at  $p < 0.05$ . **(B)**  
17  
18 Outdoor experiments. Right: photo of a 900 L controlled raceway-photobioreactor  
19  
20 (RW) used for the adhesion of *N.gaditana* produced in semicontinuous operational  
21  
22 mode. Left: photos after two months of operation after harvesting all the existing  
23  
24 microalgae culture in the RW and just after washing the RW with seawater to eliminate  
25  
26 dirt deposited on the five samples. **The values of the average surface roughness ( $R_a$ )**  
27  
28 **have been included.**  
29  
30  
31  
32  
33  
34

35 **Figure 5.** The two biocompatibility theories developed by Baier (green line) and Vogler  
36  
37 (blue lines - reproduced from Figure 10.2 of (Vogler, 2001)). The right *y*-axis shows the  
38  
39 relative strength of biological interaction, while the two *x*-axes show the degree of  
40  
41 wettability of the surfaces ( $\tau^o$ ) and the critical surface tension ( $\gamma_c$ ). Baier theory predicts  
42  
43 minimum biological interaction on hydrophobic surfaces of high water contact angle  
44  
45 ( $\theta_w \approx 105\text{-}110^\circ$ , equivalent to a  $\tau^o \approx -15 \text{ mJm}^{-2}$  according to Vogler theory) with  
46  
47 biological interactions increased for super-hydrophobic surfaces (left hand of the Baier  
48  
49 curve) and for surfaces with decreased hydrophobicity (right hand of Baier curve). On  
50  
51 the other hand, Vogler theory predicts minimum biological interaction on amphiphilic  
52  
53 surfaces ( $\theta_w \approx 65^\circ$ ;  $\tau^o \approx 35\text{-}38 \text{ mJm}^{-2}$ ). Biological interaction increases as either the  
54  
55 hydrophobicity (type I biological response) or the hydrophilicity increases (type II).  
56  
57  
58  
59  
60

1  
2  
3 704 Black circles indicate the number of cells adhered on the different surface materials  
4  
5 705 tested in the indoor experiments (left  $y$ -axis) as a function of their physico-chemical  
6  
7 706 surface properties,  $\tau^o$  and  $\gamma_c$ , (from Figure 4A). In addition, inserts indicate the values of  
8  
9  
10 707  $\gamma_c$  and  $\tau^o$  for PC-C1, SilicOne®, which showed the best antibiofouling properties in the  
11  
12 708 outdoor pilot plant experiments, before (hydrophobic) and after (amphiphilic) exposure  
13  
14 709 to natural seawater (from Figure 3B).

16  
17 710

18  
19 711

20  
21 712

22  
23 713

24  
25 714

26  
27 715

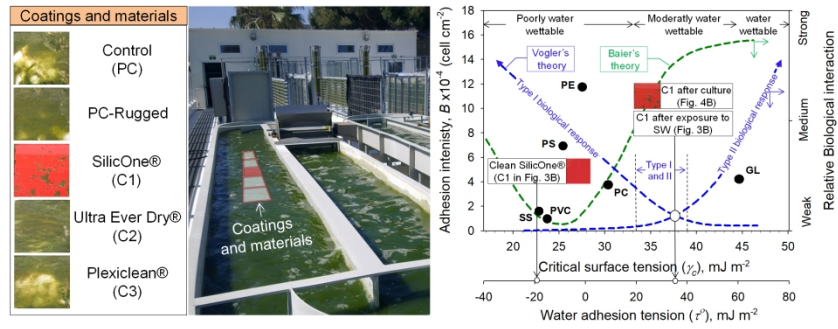
28  
29 716

30  
31 717

32  
33 718

34  
35 719  
36  
37  
38  
39  
40  
41  
42  
43  
44  
45  
46  
47  
48  
49  
50  
51  
52  
53  
54  
55  
56  
57  
58  
59  
60

GRAPHICAL ABSTRACT



254x190mm (300 x 300 DPI)



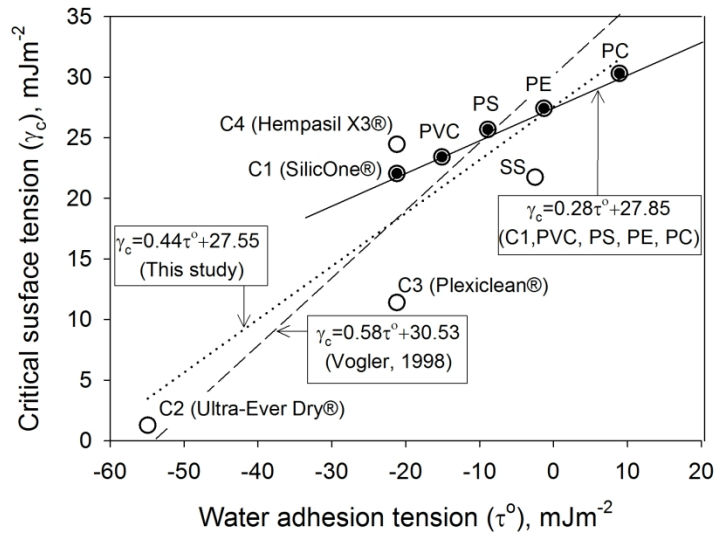


Figure 1

Comparison of the predicted relationship (dashed line) between the critical surface tension ( $\gamma_c$ ) and water adhesion tension ( $\tau^0$ ) reported by Vogler (1998) and the relationship (dotted line) obtained from the experimental data in this study (open and filled circles). The solid line indicates the relationship between  $\gamma_c$  and  $\tau^0$  for only the five polymeric and hydrophobic surfaces: (SilicOne®, PVC, PC, PS and PE – filled circles).

190x254mm (300 x 300 DPI)

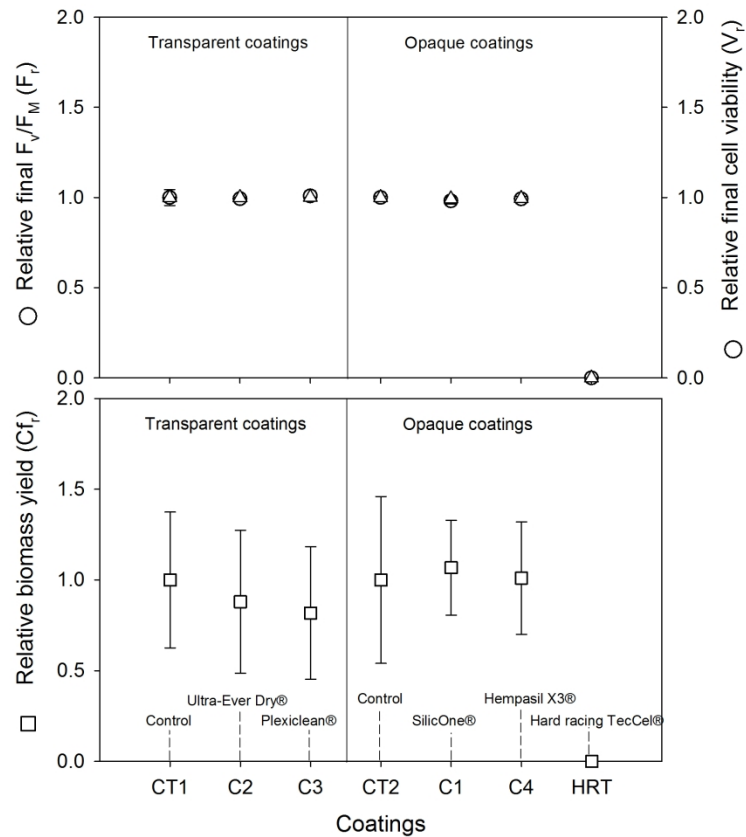


Figure 2

Evaluation of the toxicity of the coatings used based on the values of maximum photochemical yield of PSII ( $F_v/F_M$ ), cell viability ( $V_r$ ) and biomass yield ( $C_{fr}$ ) reached at the end of batch cultures, relative to corresponding values obtained from controls (CT1 and CT2). Data points are averages, and vertical bars are standard deviation (SD) for duplicate samples. Points without SD bars indicate that the SD was smaller than the symbol.

190x254mm (300 x 300 DPI)

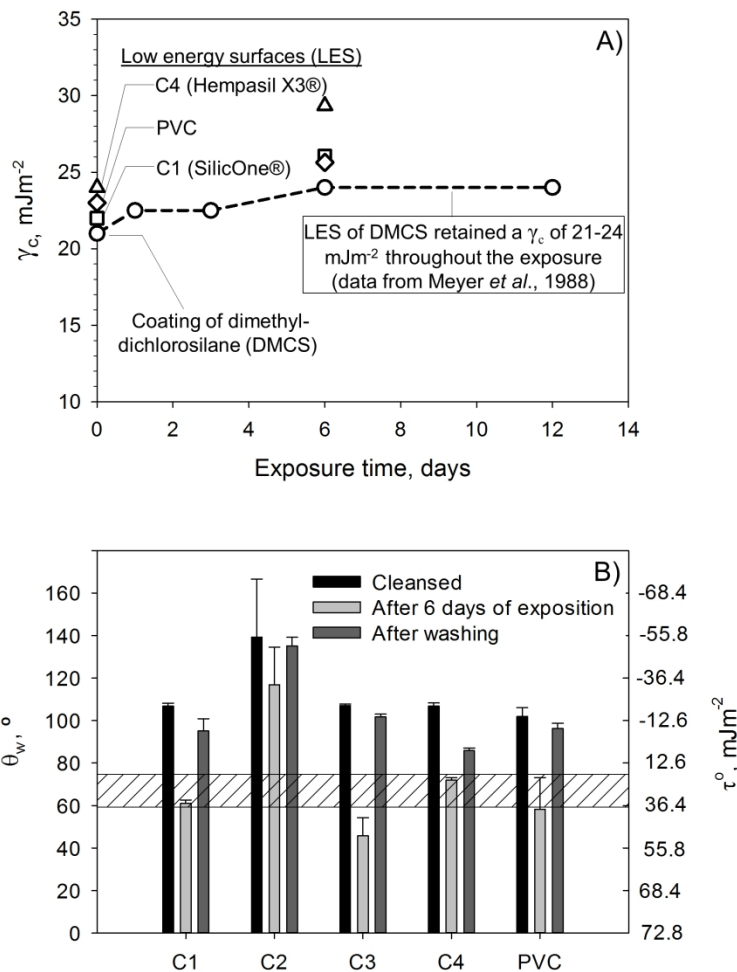


Figure 3

Effect of seawater exposure on the water adhesion tension ( $\tau^0$ ) and water contact angle ( $\theta_w$ ) of coatings and materials used. (A) Temporal evolution of the critical surface tension ( $\gamma_c$ ) of the low energy surfaces used in this study (SilicOne®, (Hempasil X3® and PVC) under exposure to seawater (empty circles and dashed line) according data reported elsewhere (Meyer et al., 1988)). (B) Measurements of  $\theta_w$  and  $\tau^0$  on PVC, PC-C2 (Ultra-Ever Dry®), PC-C3 (Plexiclean®), PC-C1 (SilicOne®) and PC-C4 (Hempasil X3®) before exposition, after 6 days of exposure to seawater and after washed with distilled water. The hatched band indicates the range of values associated with amphiphilic surfaces.

190x254mm (300 x 300 DPI)

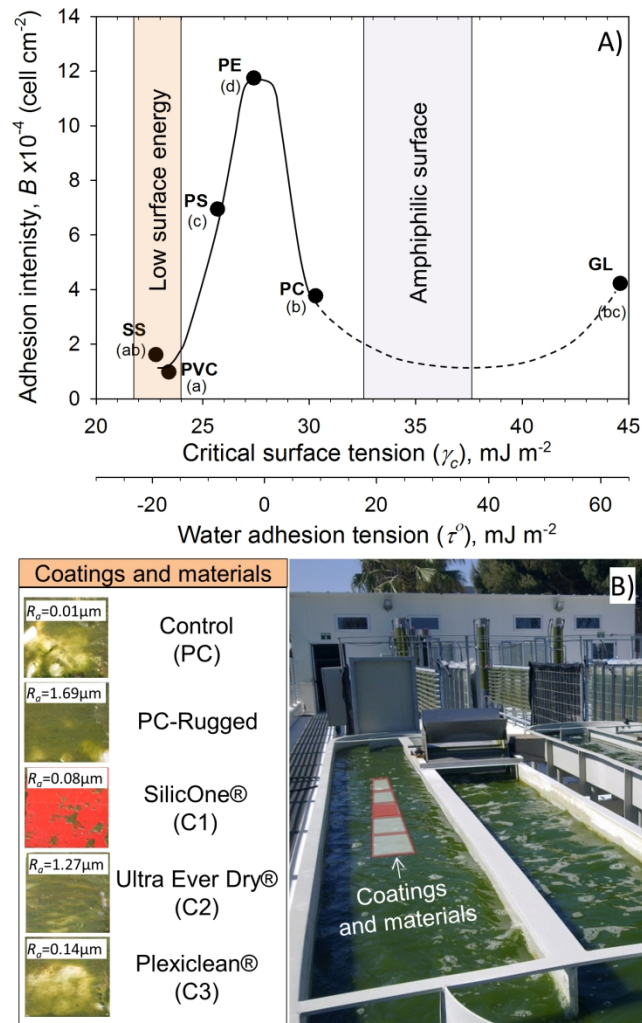
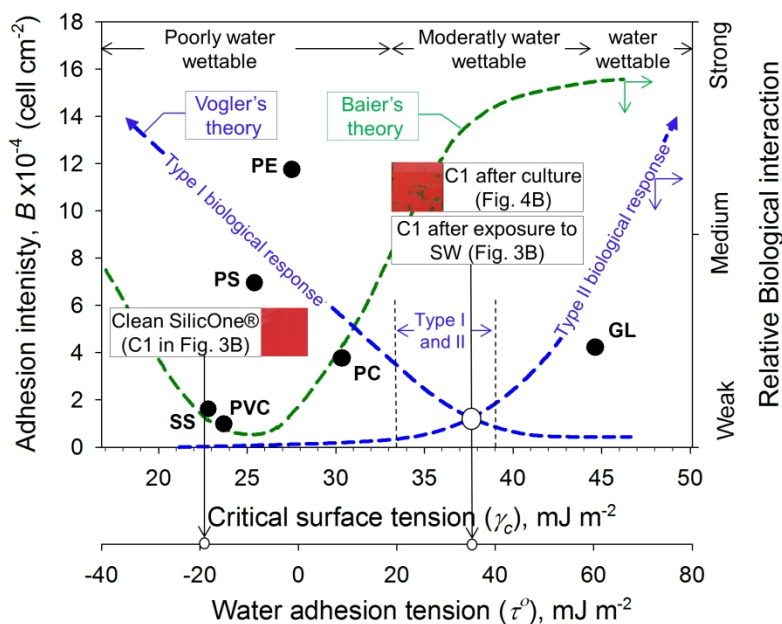


Figure 4

(A) Indoor experiments. Variation in the number of adhered cells per  $\text{cm}^2$  (B) as a function of the critical surface tension ( $\gamma_c$ ) and water adhesion tension ( $\tau^0$ ) for different materials tested in the MRD in contact with the culture of *N. gaditana*. The culture was boosted from the PBR module, operated in continuous operational mode, at a flow rate of  $25 \text{ L h}^{-1}$  providing fluid-dynamics conditions in the boundary layer of the tested materials similar to those existing in the vicinity of the wall of a tubular PBR. Lowercase letters indicate values that did not differ significantly at  $p < 0.05$ . (B) Outdoor experiments. Right: photo of a 900 L controlled raceway-photobioreactor (RW) used for the adhesion of *N. gaditana* produced in semicontinuous operational mode. Left: photos after two months of operation after harvesting all the existing microalgae culture in the RW and just after washing the RW with seawater to eliminate dirt deposited on the five samples. The values of the average surface roughness ( $R_a$ ) have been included.

190x254mm (300 x 300 DPI)



The two biocompatibility theories developed by Baier (green line) and Vogler (blue lines - reproduced from Figure 10.2 of (Vogler, 2001)). The right y-axis shows the relative strength of biological interaction, while the two x-axes show the degree of wettability of the surfaces ( $\tau^0$ ) and the critical surface tension ( $\gamma_c$ ). Baier theory predicts minimum biological interaction on hydrophobic surfaces of high water contact angle ( $\theta_W \approx 105-110^\circ$ , equivalent to a  $\tau^0 \approx -15 \text{ mJm}^{-2}$  according to Vogler theory) with biological interactions increased for super-hydrophobic surfaces (left hand of the Baier curve) and for surfaces with decreased hydrophobicity (right hand of Baier curve). On the other hand, Vogler theory predicts minimum biological interaction on amphiphilic surfaces ( $\theta_W \approx 65^\circ$ ;  $\tau^0 \approx 35-38 \text{ mJm}^{-2}$ ). Biological interaction increases as either the hydrophobicity (type I biological response) or the hydrophilicity increases (type II). Black circles indicate the number of cells adhered on the different surface materials tested in the indoor experiments (left y-axis) as a function of their physico-chemical surface properties,  $\tau^0$  and  $\gamma_c$ , (from Figure 4A). In addition, inserts indicate the values of  $\gamma_c$  and  $\tau^0$  for PC-C1, SilicOne®, which showed the best antibiofouling properties in the outdoor

1  
2  
3  
4  
5  
6  
7  
8  
9  
10  
11  
12  
13  
14  
15  
16  
17  
18  
19  
20  
21  
22  
23  
24  
25  
26  
27  
28  
29  
30  
31  
32  
33  
34  
35  
36  
37  
38  
39  
40  
41  
42  
43  
44  
45  
46  
47  
48  
49  
50  
51  
52  
53  
54  
55  
56  
57  
58  
59  
60

pilot plant experiments, before (hydrophobic) and after (amphiphilic) exposure to natural seawater (from Figure 3B).

190x254mm (300 x 300 DPI)

**Table 1.** Surface roughness, contact angles, total free surface energy components, critical surface tension, free energy of cohesion and water adhesion tension of the different substrates

	$R_a, \mu\text{m}$	Contact angles, $\theta$ ( $^\circ$ )			Surface energy components, free energy of cohesion and water adhesion tension ( $\text{mJm}^{-2}$ )						
		$\theta_W$	$\theta_F$	$\theta_D$	$\gamma_s^{LW}$	$\gamma_s^+$	$\gamma_s^-$	$\gamma_s^{AB}$	$\gamma_s^{TOT}$	$\Delta G_{coh}$	$\tau^o$
PC	0.03±0.00	83±2	67±1	57±4	30.30	0.10	6.84	2.98	31.96	-47.45	8.9
PVC	0.47±0.02	102±3	83±3	69±3	23.41	0.01	1.30	0.23	23.64	-77.46	-15.1
PS	0.03±0.00	97±2	77±0	65±1	25.68	0.83	1.83	2.45	28.15	-61.52	-8.9
PE	0.13±0.01	91±3	77±2	62±2	27.42	0.01	5.56	0.47	27.89	-53.94	-1.3
SS	0.34±0.04	92±1	80±5	72±2	21.74	0.04	6.01	0.98	22.72	-50.40	-2.5
GL	0.13±0.01	34±1	58±5	55±2	31.45	0.33	73.37	9.84	41.29	61.18	60.4
PC-C1 (SilicOne®)	0.08±0.01	107±1	90±1	72±3	22.04	0.09	1.18	0.66	22.70	-75.23	-21.2
PC-C2 (Ultra-Ever Dry®)	1.27±0.33	139±22	143±1	133±2	1.28	0.24	1.46	1.17	2.45	-95.20	-54.9
PC-C3 (Plexiclean®)	0.14±0.05	107±13	101±13	93±3	11.40	0.02	4.44	0.53	11.93	-61.30	-21.2
PC-C4 (Hempasil X3®)	0.31±0.02	107±1	88±2	67±7	24.45	0.13	0.85	0.67	25.13	-77.53	-21.2

( $R_a$ ): average surface roughness; ( $\theta$ ): the measured contact angle; ( $\gamma$ ): surface free energy; ( $\Delta G$ ): change in free energy; ( $\tau^o$ ): water adhesion tension. The subscripts:  $W, F, D, s$  and  $coh$  refer the water, formamide, diiodomethane, substrata and cohesion, respectively. The superscripts:  $LW, +, -, AB$  and  $TOT$  refer the Lifshitz-van der Waals component, electron acceptor parameter, electron donor parameter, acid-base component and total sum of the all components ( $AB, EL$ ), respectively.

## Supplementary Material

### 1. Determination of the physicochemical properties of the surfaces tested

The results from contact angle measurements and known surface tension properties of three probe liquids (W: water, D: diiodomethane, F: Formamide) are used to calculate the surface energy parameters of the substrata based on the extended Young's equation according to Eq [1]:

$$\cos(\theta_i) = -1 + \frac{2 \cdot (\gamma_s^{LW} \cdot \gamma_i^{LW})^{0.5}}{\gamma_i} + \frac{2 \cdot (\gamma_s^+ \cdot \gamma_i^-)^{0.5}}{\gamma_i} + \frac{2 \cdot (\gamma_s^- \cdot \gamma_i^+)^{0.5}}{\gamma_i} \quad [1]$$

The subscript i refer the probe liquid and s refer the substrata;  $\theta$ : The measured contact angle; ( $\gamma^{LW}$ ): The apolar (LW) Surface energy component; ( $\gamma^+$ ,  $\gamma^-$ ): The electron donor and acceptor parameters, respectively. The values of the components of the surface tension of the three test liquids used are:

$$\gamma_D = 50.8 \frac{mJ}{m^2}; \quad \gamma_D^+ = 0 \frac{mJ}{m^2}; \quad \gamma_D^- = 0 \frac{mJ}{m^2}; \quad \gamma_D^{LW} = 50.8 \frac{mJ}{m^2}$$

$$\gamma_F = 58 \frac{mJ}{m^2}; \quad \gamma_F^+ = 2.28 \frac{mJ}{m^2}; \quad \gamma_F^- = 39.6 \frac{mJ}{m^2}; \quad \gamma_F^{LW} = 39 \frac{mJ}{m^2}$$

$$\gamma_W = 72.8 \frac{mJ}{m^2}; \quad \gamma_W^+ = 25.5 \frac{mJ}{m^2}; \quad \gamma_W^- = 25.5 \frac{mJ}{m^2}; \quad \gamma_W^{LW} = 21.8 \frac{mJ}{m^2}$$

The contact angles measured with the diiodomethane are used to solve apolar component ( $\gamma_s^{LW}$ ) of the surface energy (Eq. [1]), and, the contact angles measured with the other two probe liquids, water and formamide, are used to solve for the other two unknown surface energy parameters, ( $\gamma_s^+$ ) and ( $\gamma_s^-$ ) (Eq. [1]). Polar surface energy component ( $\gamma_s^{AB}$ ) of the surface is calculated based on the calculated ( $\gamma_s^+$ ) and ( $\gamma_s^-$ ) (Eq. [2]). The total surface energy ( $\gamma_s^{TOT}$ ) is calculated based on ( $\gamma_s^{AB}$ ) and ( $\gamma_s^{LW}$ ) (Eq. [3]).

$$\gamma_s^{AB} = 2 \cdot \sqrt{\gamma_s^+ \cdot \gamma_s^-} \quad [2]$$

$$\gamma_s = \gamma_s^{AB} + \gamma_s^{LW} \quad [3]$$



## 2. Degree of hydrophobicity and hydrophilicity of the surfaces tested

The hydrophobicity and hydrophilicity of surfaces are determined based on the free energy of cohesion  $\Delta G_{coh}$  according to Eq. [4],

$$\Delta G_{coh} = -2 \cdot (\sqrt{\gamma_s^{LW}} - \sqrt{\gamma_W^{LW}})^2 - [4(\sqrt{\gamma_s^+ \cdot \gamma_s^-} + \sqrt{\gamma_W^+ \cdot \gamma_W^-} - \sqrt{\gamma_s^+ \cdot \gamma_W^-} - \sqrt{\gamma_s^- \cdot \gamma_W^+})] \quad [4]$$

While a negative  $\Delta G_{coh}$  indicates hydrophobicity, a positive value indicates hydrophilicity.

## 3. Determination of the Van Der Waals component of the change in free energy of adhesion

The LW component of surface free energy of particles ( $\gamma_p^{LW}$ ), aqueous medium ( $\gamma_W^{LW}$ ) and substrate ( $\gamma_s^{LW}$ ) are taken into account to calculate LW component of the change in free energy of adhesion (Eq.[5]).

$$\Delta G_{adh}^{LW} = -2 \cdot (\sqrt{\gamma_p^{LW}} - \sqrt{\gamma_W^{LW}}) \cdot (\sqrt{\gamma_s^{LW}} - \sqrt{\gamma_W^{LW}}) \quad [5]$$

While a negative  $\Delta G_{adh}^{LW}$  indicates adhesion, a positive value indicates repulsion between the substrata and particle.